International Review of Hydrobiology 2016, *101*, 1–12 DOI 10.1002/iroh.201501811

RESEARCH PAPER

Stratification and residence time as factors controlling the seasonal variation and the vertical distribution of chlorophyll-*a* in a subtropical irrigation reservoir

José Gabriel León[1,2], *Sara Guadalupe Beamud*[3], *Pedro Félix Temporetti*[3], *Adrián Gonzalo Atencio*[2], *Mónica Mabel Diaz*[3] *and Fernando Luis Pedrozo*[3]

[1] Instituto Argentino de Nivología, Glaciología, y Ciencias Ambientales (IANIGLA), Mendoza, Argentina
[2] Departamento General de Irrigación, Gobierno de Mendoza, Mendoza, Argentina
[3] Instituto de Investigaciones en Biodiversidad y Medio Ambiente (INIBIOMA), CONICET – Universidad Nacional del Comahue, S. C. de Bariloche, Argentina

Received: August 20, 2015
Revised: November 30, 2015
Accepted: February 9, 2016

Reservoir trophic state is controlled by light and nutrient availability, as well as by hydraulic management and stratification pattern. In arid zone reservoirs, the inflow and outflow discharges have extreme seasonal variations which produce well-defined cycles of filling and draining. Moreover, since stratification often occurs, epilimnion and hypolimnion renewal rates may vary producing different environmental conditions throughout the water column. These variation patterns may affect phytoplankton growth at both temporal and spatial scales. For two hydrological years, we analyzed the influence of light climate, nutrients, residence time (Tw), and stratification on phytoplankton biomass (as chlorophyll-***a*** [Chl-***a***]) in an irrigation reservoir (276 hm^3) in the arid central Andes in Argentina (33°S). The reservoir was turbid (Z_{Secchi}: 1.4 m) with relatively high levels of dissolved nitrogen and phosphorus (60 $\mu g P L^{-1}$ and 560 $\mu g N L^{-1}$, respectively). Stratification occurred from mid-spring to late-summer, when hypolimnetic oxygen and pH decreased whereas dissolved nutrients increased. The reservoir was mesotrophic (Chl-***a***: 4.6–10.8 $\mu g L^{-1}$) and showed two semi-annual peaks of Chl-***a*** (summer and winter). Depending on the water column circulation, Chl-***a*** was directly related to Tw for $60 > Tw > 200$ and inversely to ammonia, during mixing and stratification periods, respectively. Phytoplankton development was strongly influenced by the seasonal variations of inflow/outflow and stratification. Chl-***a*** peaked in summer, when inflow plunged into the hypolimnion of the stratified reservoir and in the warm and mixed epilimnion algae proliferated until nutrients depletion. Alternatively, the winter Chl-***a*** maximum is likely to be produced by the higher concentration of nutrients combined with the turbulent mixing in the water column which acts as a mechanism that helps to overcome light-limitation. Since stratification modifies the vertical distribution of Tw, the use of a single annual value of this hydraulic parameter to assess its effect on the reservoir trophic state results inadequate. This paper constitutes the first description of hydrologic effects on Chl-***a*** dynamics in a reservoir in arid central western Argentina.

Keywords:
Hydraulic residence time / Nutrients / Reservoir / Stratification / Trophic state

Handling Editor: Rita Adrian

Correspondence: José Gabriel León, Instituto Argentino de Nivología, Glaciología, y Ciencias Ambientales (IANIGLA), CCT-CONICET Mendoza. Av. R. Leal s/n (5500) Mendoza, Argentina
E-mail: jleon@mendoza-conicet.gob.ar
Fax: 54-261-5242001

Abbreviations: ECR, El carrizal reservoir; Tw, residence time; RWCS, relative water column stability; TDS, total dissolved solids; EC, electrical conductivity; SRP, soluble reactive phosphorus; DIN, dissolved inorganic nitrogen

1 Introduction

Biological processes in reservoirs are driven by the physical and geochemical factors that result from their condition as a hybrid between a lake and a river (Kimmel et al., 1990). Among the factors controlling trophic state, horizontal transport is usually represented by the hydraulic residence time (Tw) and is often assumed to be inversely related to phytoplankton abundance due to advective

losses in high flow conditions (Lucas et al., 2009) and to its effects on light and nutrients availability (Rangel et al., 2012; Rigosi & Rueda, 2012; Cunha et al., 2013). Moreover, in thermally stratified reservoirs, another source of variability is introduced: As water renewal rate decreases, the epilimnion may constrain algal growth by nutrients depletion and self-shading (Hu et al., 2016). Similarly, during water column mixing, algal assembly is likely to be light limited due to lower radiation incidence and lower exposure of algae to optimal light conditions (Becker et al., 2010).

In arid climate zones, the inflow and outflow discharges of reservoirs are highly variable on a seasonal basis (Naselli-Flores, 2003; Zohary & Ostrovsky, 2011) resulting in intra-annual Tw oscillations. This "hydraulic duality" was implicitly stated in the concept developed by Søballe and Kimmel, (1987), who established a threshold value of 60–100 days for Tw, below which the horizontal transport typical of a river controls phytoplankton growth by means of advective losses. Above this threshold, the limnetic primary production is controlled by factors characteristic of a lacustrine environment, such as light and nutrient availability and trophic interactions. Furthermore, stratification may decouple vertical circulation, producing epilimnion and hypolimnion renewal rates that differ, thus affecting algal growth at a temporal and spatial scale (Marcé et al., 2006).

In order to establish the influence of physical and chemical factors on temporal and spatial variability of chlorophyll-***a*** (Chl-***a***), we studied the limnological features of a subtropical reservoir in arid central western Argentina for two hydrological years. We hypothesized that the combination of successive filling and draining periods with seasonal stratification produces alternate states that have contrasting physical and chemical conditions which control Chl-***a*** through phytoplankton access to light and nutrients.

2 Materials and methods

2.1 Study area

The hydrographic basin of El Carrizal Reservoir (ECR) (14 040 km^2) is located in the eastern slope of the South Central Andes (Fig. 1). The reservoir is mainly fed by River Tunuyán (average discharge 35 m^3 s^{-1}), which, in turn, is fed almost exclusively by snow and glacier melting (Masiokas et al., 2010). The basin area upstream from the dam can be divided into two different subunits considering topography, lithology, and human activities. One is the river headwater in the mountain region (>1200 m asl), which is characterized by steep slopes, high content of sedimentary rocks, marked seasonal flow,

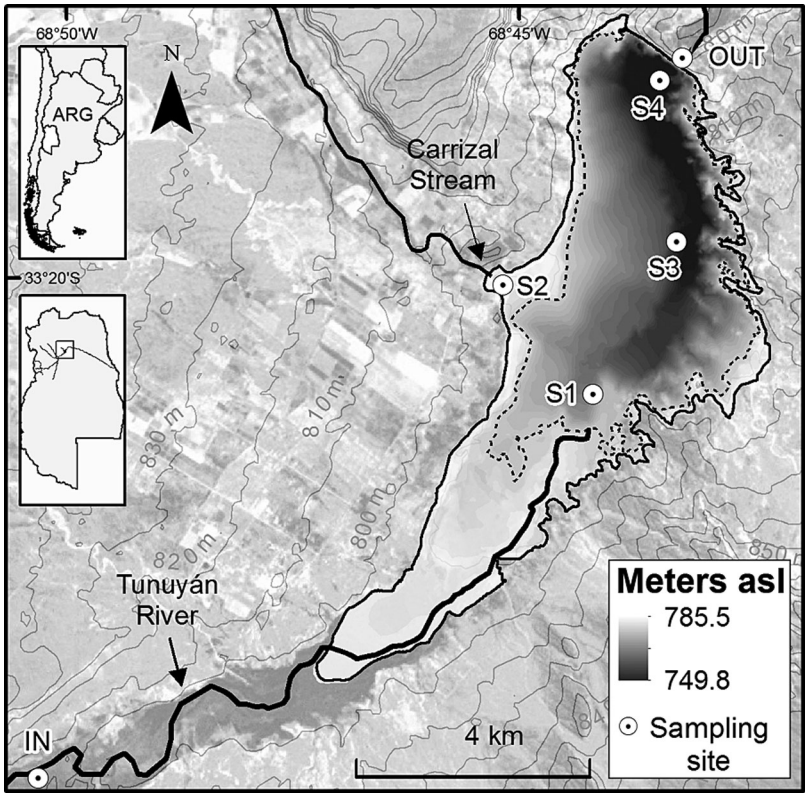

Figure 1. Sampling sites location in El Carrizal Reservoir. The dotted contour line indicates the shoreline at the annual average water level (781.6 m asl) for the studied period (2009–2011).

and scarce human presence (León & Pedrozo, 2015). The other subunit is located downstream (790–1200 m asl), where there is an irrigation oasis that is crossed by a number of relatively dilute streams, which are channelized for distribution (León, 2013). The climate in the region is classified as cold desert (BWk) according to Köppeńs classification.

The maximum depth of the reservoir is 40 m, its mean depth is 9 m, and its volume at maximum water level (785.5 m asl) is 275.6 hm^3. The inflow (1100 $hm^3\,y^{-1}$) annual hydrograph has two peaks (Fig. 2): A large one during the snow melting season (September–February) and a small one between late autumn and early winter (May–July). A second tributary of the reservoir is Stream Carrizal, which drains an agricultural area (840 km^2) and provides *ca*. 28 $hm^3\,y^{-1}$. The reservoir outlet is fixed and located at the base of the dam (749 m asl).

2.2 Field sampling and sample analysis

Water samples were collected monthly from March 2009 to March 2011 at sites inflow (IN) and outflow (OUT), and at four other predetermined sites inside the reservoir (S1–S4, Fig. 1) between 10:00 am and 14:00 pm, recording maximum depth (Z_{max}) and Secchi disk depth (Z_{SD}) at each site. The location of each site was selected considering longitudinal river-reservoir gradients (Thornton, 1990); sites IN, OUT, S1, and S2 were considered to be influenced by the river environment, while sites S3 and S4 were considered to represent the reservoir limnetic zone. Sub-surface samples (0.5 m) were collected in all sites (S1_0.5 m to S4_0.5 m). S3 and S4 were also sampled at 10 m (S3_10 and S4_10 m), and S4 at ~1 m above the bottom sediment (S4_Z_{max}–1 m). Euphotic zone height (Z_{Eu}) was estimated as Z_{SD}*2.7 (Padisák, 2005). Thermocline depth (Z_{mix}) was determined from the temperature profiles at site S4 ($>1°\,C\,m^{-1}$). Water samples were collected with a Van Dorn bottle and analyzed in situ for: Temperature (Temp), pH, electrical conductivity (EC), and dissolved oxygen (DO) using Thermo Orion 230A (T° and pH), WTW Multiline P4 (EC) and Thermo-Orion Star3 (DO) instruments. Samples were stored into 3.5 L PVC bottles prewashed with deionized water ($<2\,\mu S\,cm^{-1}$) and rinsed with the sampled water. Samples were taken to the laboratory refrigerated and in the dark, filtered within 4 h after collection, and analyzed in duplicate within 24 h. Suspended particulate matter (SPM) was determined at IN, OUT, and S4_0.5 m by mass difference in pre-calcined (500°) 0.7 μm pore glass fiber filters dried to constant mass. Total dissolved solids (TDS) were estimated in 0.45 μm filtered water evaporated at 180° C. Total and dissolved nutrients were determined spectrophotometrically in compliance with APHA (1998): Soluble reactive phosphorus (SRP) was estimated by the ascorbic acid method; nitrate (NO_3^-) was determined by cadmium column reduction followed by diazotization with sulfanilamide; ammonia (NH_4^+) was estimated by the phenate method; nitrite (NO_2^-) was determined by diazotization with sulfanilamide. Dissolved inorganic nitrogen (DIN) available for algal consumption was estimated as the sum of the three nitrogen species ($DIN = NO_3^- + NH_4^+ + NO_2^-$). Soluble reactive silica (SRSi) was determined in summer 2011 ($n = 5$) at sites IN, S4_0.5m, and OUT, by the silicomolybdate method. Total phosphorus (TP) was determined by autoclave acid digestion with $K_2S_2O_8$, followed by SRP determination, and total nitrogen (TN) by autoclave basic digestion with $K_2S_2O_8$ followed by NO_3^- determination. TP and TN were determined in an unfiltered sample and the rest of the analytes in filtered water (0.45 μm, cellulose acetate). For Chl-***a*** determination, 0.5 L sub-samples were filtered through 0.7 μm pore size glass fiber filters and extracted in neutralized 90% acetone at 4°C for 24 h in darkness.

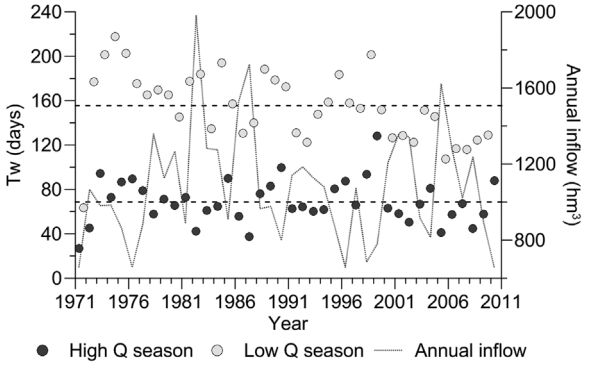

Figure 2. Semi-annual time series (1971–2011) of hydraulic residence time (Tw) in El Carrizal reservoir considering the high and low flow-through periods (High Q season: November–March; Low Q season: April–October). Tw was calculated from daily averages of hydraulic parameters and assuming continuously stirred tank reactor conditions (see text). Annual inflow volume is also shown. Dashed horizontal lines indicate the Tw historical average for periods of Low Q (154 days) and High Q (69 days).

2.3 Meteorological and hydraulic data

Daily average incident solar irradiance (300–3000 nm) was measured with a thermoelectric transducer (SIAP + MICROS t055) at the Junín meteorological station, located at 20 km NE of the reservoir (DACC, 2011). The incident photosynthetically active radiation (PAR, 400–700 nm) was estimated as 45 of 96% of the incident solar irradiance since it is considered that 4% of the latter is reflected by water (Domingues et al., 2012). Hourly data on wind speed

and direction were obtained from the San Martin meteorological station, located at 32 km NE of the reservoir (SMN, 2011). Rainfall averages *ca*. 150 mm y^{-1} and is concenterd in summer. Local precipitation is expected to scarcely contribute to river runoff, as reflected in the low specific discharge at the reservoir inflow (20 mm y^{-1}) compared to that of headwaters (380 mm y^{-1}).

Daily average inflow and outflow discharge is routinely measured by the local water authority at 5 km upstream ECR and at its withdrawal, respectively (Fig. 1). The relative water column stability (RWCS) was used to assess stratification, which was considered to occur at RWCS > 50 (Padisák et al., 2003):

$$\mathrm{RWCS} = \frac{\rho_{Zh} - \rho_{Z=0}}{\rho_{4^\circ} - \rho_{5^\circ}}$$

where ρ is water density: ρ_{Zh}, at hypolimnion (between 20 and 30 m in this study); $\rho_{Z=0}$, at surface; ρ_{4°, pure water at 4°C; and ρ_{5°, pure water at 5°C. For this calculation, ρ was estimated at sites IN, OUT, and S4 (Fig. 1) from temperature, TDS, and SPM using formulae in Ji (2008). For density calculation purpose, the SPM concentration at S4_Z_{max}–1 m was considered to be equivalent to that of site OUT.

Daily Tw was estimated as the ratio between the reservoir volume and its volumetric flow rate (Straškraba & Hocking, 2002):

$$\mathrm{Tw} = \frac{V}{(Q_{in} + Q_{out})/2}$$

where V is the volume in the reservoir and Q_{in} and Q_{out} are the inflow and outflow discharges, respectively. In mixed water columns, this Tw estimation method is preferred to simple volume quotient ($\mathrm{Tw} = V/Q_{out}$) because the former considers both inflow and outflow discharges to act on reservoir water movement (Andradóttir et al., 2012). The volume and discharge values utilized for Tw estimation in each sampling date corresponded to 10-day average values prior to sampling.

Differences and similarities between datasets were evaluated by the Kruskal–Wallis test and pair comparison. Correlations between water features were assessed by the Spearman coefficient (R_S). Spatial grouping of sites was explored by principal component analysis. All analyses were performed by using INFOSTAT software (Di Rienzo et al., 2013).

3 Results

In ECR, the predominant winds came from SW and SE, and showed a daily pattern of direction and intensity change; from SW in the morning, rotating and intensifying to SE in the evening. Although the wind speed exceeded 5 m s^{-1} *ca*. 10% of the time, the daily average for 2009–2011 was moderate (1.8 m s^{-1}).

The annual Tw in ECR was calculated by considering the mean annual volume in the reservoir (194 hm^3) and the inflow discharge (1100 $hm^3\,y^{-1}$), resulting in a value of 62 days. However, when considering the short-term hydraulic operation, it becomes apparent that the seasonal flow-through distribution is not homogeneous (Fig. 2). In 2009–2011, ECR stratified (RWCS >50) from mid-spring to late-summer and the daily Tw ranged from 30 to 324 days. ECR volume varied between 94.6 and 275.6 hm^3, displaying two semi-annual filling and draining

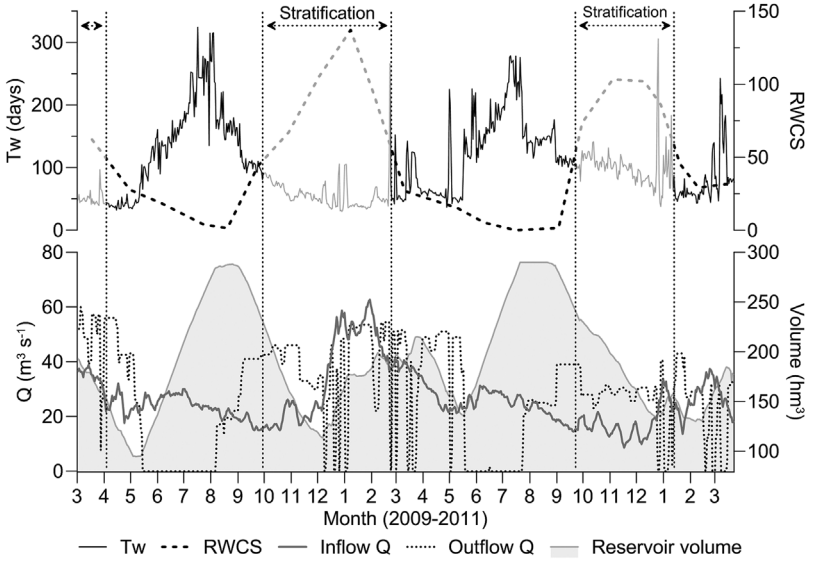

Figure 3. Inflow and outflow mean daily discharge (Q), volume, and the stratification period in El Carrizal Reservoir during 2009–2011. In this figure, the hydraulic residence time (Tw) plot corresponds to continuously stirred tank reactor (CSTR) conditions, and therefore Tw during stratification is indicated as a dim line (see text).

periods producing two peaks: One large and narrow in late winter, and another one short and wide in summer. The winter maximum was due to outflow cessation and occurred during the season of low inflow discharge, when the river merged into the cold and mixed reservoir (Figs. 3 and 4). Then, after nearly one month at maximum volume and mixed water column, the draining period started and lasted until mid-spring, well after stratification onset. During late-spring and summer, when inflow discharge increased due to snow-melting, the inflow/outflow surplus produced another filling phase. In autumn, the second draining period occurred entirely when water column is mixed.

The average inflow discharge during the 2009–2010 hydrological year was higher than that in 2010–2011 ($Q_{2009–2010} = 29.5\,m^3\,s^{-1}$, $Q_{2010\text{-}2011} = 23.7\,m^3\,s^{-1}$, $p < 0.001$, $n = 365$), when the overall EC in the reservoir exhibited higher values ($EC_{2009–2010} = 1123\,\mu S\,cm^{-1}$, $Q_{2010–2011} = 1362\,\mu S\,cm^{-1}$, $p < 0.01$, $n = 11$). EC was the only variable found to be affected by discharge decrease since neither the nutrients concentrations nor the epilimnetic Chl-***a*** concentrations in reservoir differed

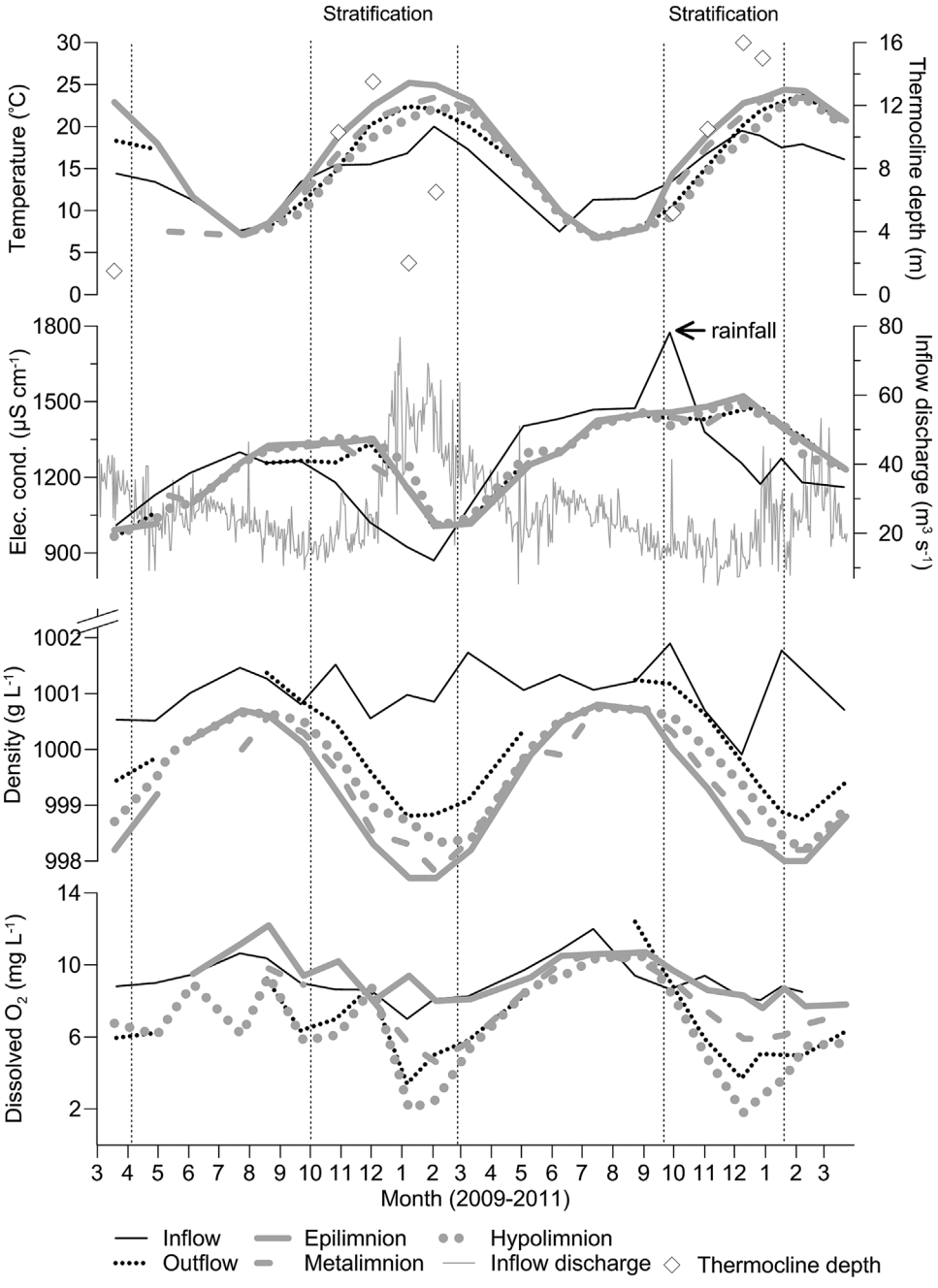

Figure 4. Dynamics of physical variables during 2009–2011 at El Carrizal Reservoir inflow (IN), outflow (OUT), and in the water column in the limnetic zone (Epilimnion, Metalimnion, and Hypolimnion corresponding respectively to depths 0.5 m, 10 m, and Z_{max}–1 m). Sites 0.5 and 10 m are spatial averages of sites S3 and S4. The arrow in the EC plot indicates a sampling date preceded by rainfall (see text). Stratification periods are indicated by dotted vertical lines and correspond to dates when relative water column stability index (RWCS) was >50.

between hydrological years ($p > 0.05$). It is noteworthy that in a shorter timescale the inflow dissolved composition was affected by rainstorms (Fig. 4), which occasionally reached *ca*. 40 mm d^{-1}. The SPM concentration (not shown) had definite spatial and temporal patterns; it was higher at IN (1076 mg L^{-1}, $n = 22$) and lower at S4_0.5 m (6 mg L^{-1}, $n = 22$) and OUT (17 mg L^{-1}, $n = 18$), and it was more variable at IN ranging from 5966 to 19 mg L^{-1} during the high and low discharge periods, respectively. The average TDS and EC did not differ among sites IN, S4_0.5 m, and OUT (>0.05, $n = 22$). TDS (not shown) ranged from 613 to 1138 mg L^{-1} and peaked at IN (1275 mg L^{-1}) after heavy rainfall. EC inside the reservoir (900–1500 μS cm^{-1}) was directly related to TDS ($R_S = 0.87$, $p < 0.001$, $n = 61$). This variable was inversely associated to inflow discharge at site IN ($R_S = -0.53$, $p < 0.05$, $n = 22$) and showed a small delay among IN and limnetic zone sites.

In both hydrological years the stratification period occurred approximately between October and February (Fig. 4). The horizontal gradient of temperature reached the maximum in mid-summer simultaneously with the highest inflow and outflow discharges. Thermocline (1–16 m) was generally deeper when epilimnion was warmer. The density difference was highest among inflow and limnetic zone sites during stratification due to the combination of high SPM and low Temp at site IN. During that period, the denser intrusion is likely to be negatively buoyant and sink to the bottom of the reservoir. Dissolved oxygen and pH exhibited a coupled behavior, both in time and space; surface sites showed smoother variations and higher pH and DO concentrations, while deep sites (10 m and Z_{max}–1 m) were less alkaline and oxygenated, and sharply decreased during stratification.

Nutrient concentrations at IN (Fig. 5) tended to be higher and more variable (coefficient of variation [CV] *ca*. 60%) than those sites inside the reservoir (S1–S4) and at OUT (CV *ca*. 40%). Surface concentrations of TP and TN were distributed homogeneously and their dissolved fractions were SRP: 24% and DIN: 67%, respectively, the latter being mostly composed of NO_3^- (*ca*. 88%). SRSi was relatively homogeneous and averaged 17, 15, and 15 mg L^{-1} at IN, S4_0.5 m, and OUT, respectively ($n = 5$). Sites S1 and S2 appeared to be influenced by tributaries as they showed higher nutrient concentrations than sites S3 and S4. Epilimnion (S3_0.5 and S4_0.5 m) and hypolimnion (S4_10 and S4_10 m) were spatially homogeneous and no significant differences were found for any variable in the mixing and stratification periods for both depths of 0.5 and 10 m. The deepest stratum (S4-Z_{max}–1 m) tended to have a higher concentration of nutrients and was lower in temperature, pH, DO, with similar values to those at OUT. Average values of epilimnetic TN:TP and DIN:SRP ratios (mass) were *ca*. 3 (1–8) and *ca*. 8 (2–26), respectively, and the lowest epilimnetic DIN:PRS ratio (<6) was recorded during stratification. At site S2, DIN:SRP ratio had higher values (DIN:SRP = 10, $p < 0.05$, $n = 21$) and higher Chl-***a*** (>40 μg L^{-1}) was observed. Water column transparency (Z_{SD}, not shown) was relatively low, averaging 1.4 m during stratification and 1.2 m during mixing. The average Z_{Eu}:Z_{mix} ratio during stratification was 0.5 ($n = 18$); i.e., 50% of euphotic zone was completely mixed, whereas during the mixing period, the Z_{Eu}:Z_{mix} ratio was 0.1 ($n = 26$). Incident PAR varied between 22 and 170 W m^{-2}, and showed higher and lower values during stratification and mixing, respectively. Chl-***a*** experienced four peaks which coincided with the stratification and mixing periods. The epilimnetic Z_{SD}, Chl-***a***, and SPM were closely related ($R_S = 0.71$, $p < 0.05$) and did not differ between stratification and mixing ($p > 0.05$). TP concentration in ECR indicated a hypereutrophic state at all sites while Chl-***a*** concentration was in the mesotrophic range, except for S2–0.5m, which was eutrophic (Fig. 6). Overall Chl-***a*** concentration was unrelated to nutrient concentration, however, when considering the stratification period, epilimnetic Chl-***a*** showed to be inversely associated to NH_4^+ (Fig. 7a; $R_S = -0.67$, $p < 0.01$, $n = 18$). Similarly, Chl-***a*** was unrelated to Tw when the entire year was considered but, when only the mixing period was taken into account, Chl-***a*** variations were directly correlated to Tw between 70 and 200 days (Fig. 7b; $R_S = 0.62$, $p < 0.001$, $n = 28$).

Spatial variability during mixing and stratification was explored by inter-site comparisons; sites S1 and S2 were excluded due to the tributary influence and S3 and S4 values for the same depth were averaged, since no difference was found among sites of equal depth. Inside the reservoir, EC did not differ among sites in either the mixing and stratification periods ($p > 0.05$). During mixing, Temp, water density, and Chl-***a*** showed no significant differences among sites and depths ($p > 0.05$); while during stratification, TN did not vary among sites and depths, and the rest of the variables considered were grouped as: IN, epilimnetic (S3_0.5 m and S4_0.5 m), metalimnetic (S3_10 m and S4_10 m), and hypolimnetic zones (S4_Z_{max}–1 m and OUT). These last two sites, together with IN, had comparable Temp during stratification, colder than at epilimnetic sites.

Site grouping can be visualized by plotting sites in the first factorial plane of principal component analysis (Fig. 8), which explains 80.5% of this variation and reveals well-defined spatial patterns. Axis 1 (47.1%) was inversely related to Temp and Chl-***a*** and directly to SRP, NH_4^+, and TP. Sites IN, S4_Z_{max}–1 m, S1_0.5 m, and OUT were directly related to this axis whereas the sites in the limnetic environment were inversely related. Axis 2 (33.4%) was positively correlated to DO, pH, EC, and Chl-***a*** and therefore surface sites showed higher values along this

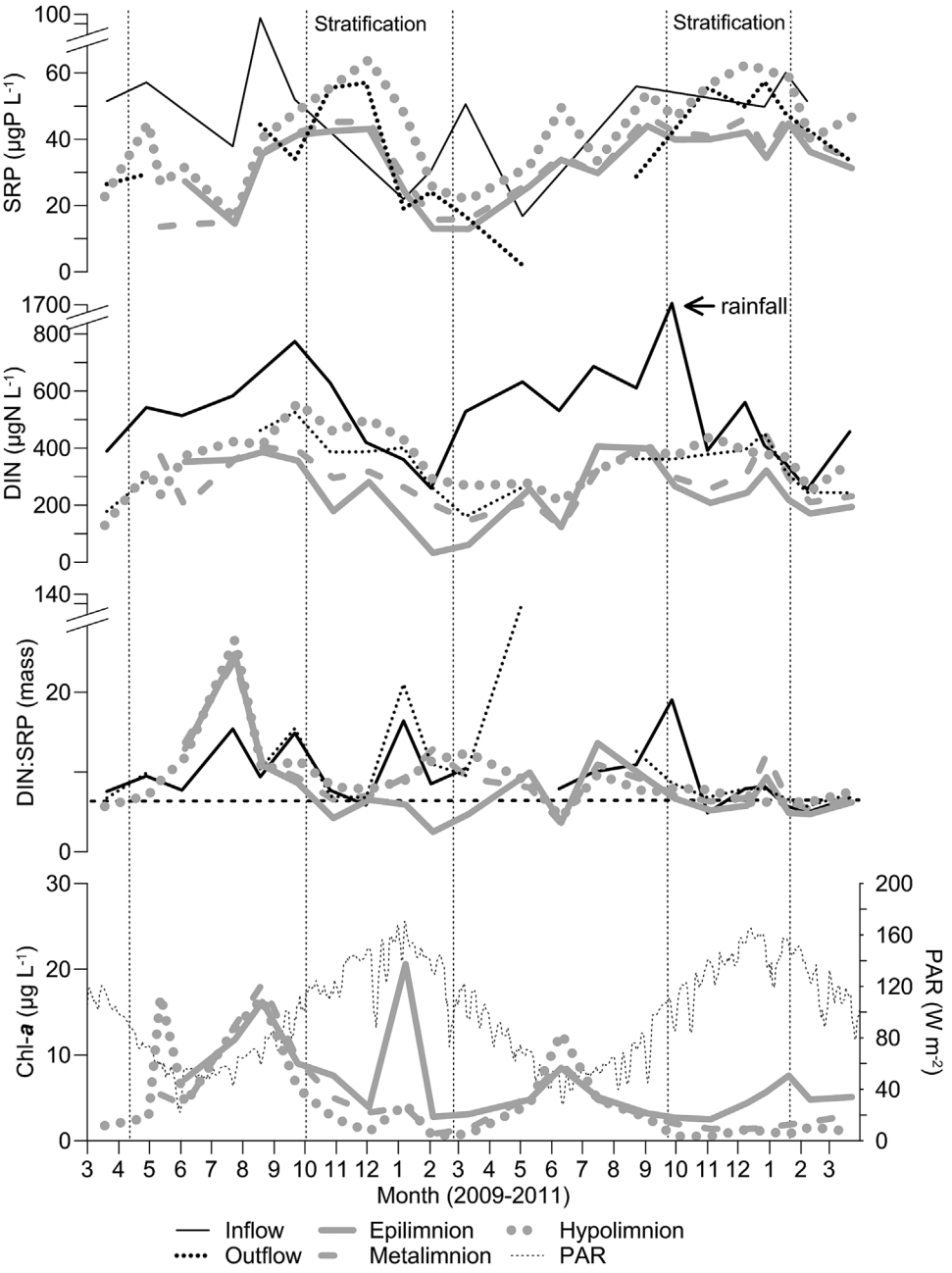

Figure 5. Dynamics of dissolved phosphorus (SRP), dissolved inorganic nitrogen (DIN), DIN:SRP ratio, chlorophyll-***a*** (Chl-***a***), and photosynthetic active radiation (PAR) during 2009–2011 at El Carrizal Reservoir inflow (IN), outflow (OUT), and in the water column in the limnetic zone (Epilimnion, Metalimnion, and Hypolimnion corresponding, respectively, to depths 0.5 m, 10 m, and Z_{max}–1 m). Sites 0.5 and 10 m are spatial averages of sites S3 and S4. The arrow in DIN plot indicates a sampling date preceded by intense rain (see text). Horizontal dashed line on DIN:SRP axis indicates DIN:SRP = 7.

axis. The most noticeable feature was the closeness between 0.5 and 10 m depth for both S3 and S4, and between OUT and S4_Z_{max}–1 m.

4 Discussion

El Carrizal reservoir is a temperate monomictic reservoir stratifying during mid-spring and mid-summer. The period studied in this paper included two hydrological years that were comparable regarding their limnological features. This condition enables exploring the relationships between the patterns of filling/draining and inflow quantity and quality seasonal variability (Figs. 3–5) to look for controlling factors of the primary productivity process in the reservoir limnetic environment. The qualitative and quantitative effects of zooplankton grazing on the abundance and composition of phytoplankton may be significant (Reynolds, 2006). However, this would not be the case of ECR, where zooplankton consists of small dimensions species indicators of eutrophication and high water renewal rates, such as *Bosmina* sp. (León, 2013),

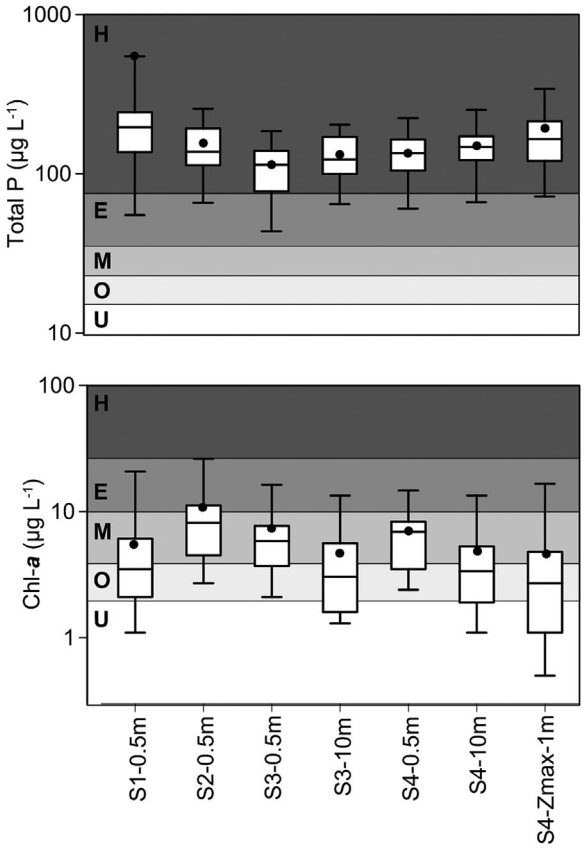

Figure 6. Trophic classification of El Carrizal reservoir (see Fig. 1 for sites location) following the criteria of Cunha et al. (2013) for tropical and subtropical reservoirs considering chlorophyll-***a*** (Chl-***a***) and total phosphorus (TP) concentrations. Trophic state ranges are: H, hypereutrophic; E, eutrophic; M, mesotrophic; O, oligotrophic; and U, ultraoligtrophic. For each site the trophic state is indicated by the red dot (geometrical mean; $n = 22$). Box: median and quartiles, and whiskers: 5 and 95 percentiles.

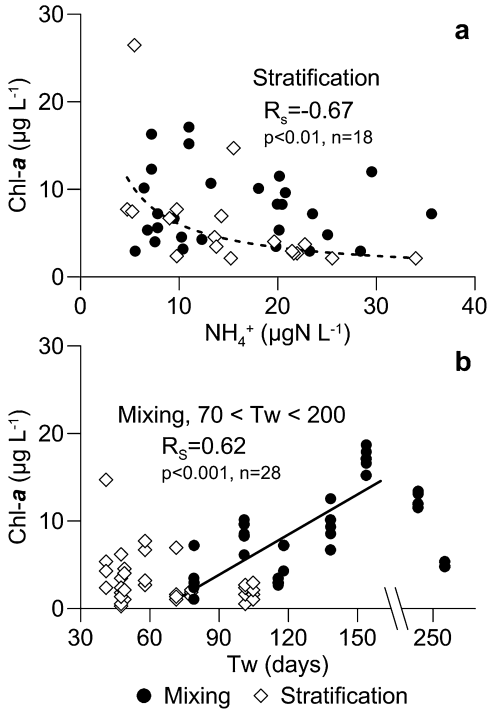

Figure 7. Covariation of chlorophyll-***a*** (Chl-***a***) in El Carrizal Reservoir. a) Epilimnetic Chl-***a*** versus nitrogen ammonia concentration (NH_4^+). Spearman correlation coefficient (RS) corresponds to stratification dataset; b) Epi and hypolimnetic Chl-***a*** versus hydraulic residence time (Tw) in whole water column. RS corresponds to the dataset of the mixing period and Tw values between 70 and 200 days.

which exerts little pressure on the major phytoplankton groups. Moreover, fish assemblage in ECR is dominated by *Odontesthes bonariensis* (Argentinean silverside: Atherinopsidae), a visual planktivorous fish which strongly controls zooplankton abundance in reservoirs maintaining it at low densities (Quirós & Boveri, 1999) and favouring "Bottom-up" processes to control algal abundance (Carpenter et al., 1987).

4.1 Physical factors

In response to wind-induced surface water movement, significant vertical transport may be produced by the counter current in the bottom layer (Ji, 2008). Although the critical speed and duration of wind maintaining stratification is a function of morphometric and environmental factors (Elçi, 2008), it is usually considered that wind-induced movement of the boundary surface layer begins at 2–3 $m\,s^{-1}$ and strong winds are assumed to occur from 5 $m\,s^{-1}$ (Antenucci & Imerito, 2000). In our study, the thermocline formation and persistence through the spring–summer period suggest that the low frequency of strong winds occurrence (during $<$10% of the time winds are $>5\,m\,s^{-1}$) is likely to be low enough so as not to break stratification permanently. On the contrary, mild wind may contribute to epilimnion formation by surface heat distribution (Wüest & Lorke, 2003). Nevertheless, short-term effects on water column circulation can be expected since the wind speed was $>5\,m\,s^{-1}$ 10% of the time, e.g., during Fohen-type wind events (locally called Zonda), when the speed can reach up to 20 $m\,s^{-1}$ for several hours. However, due to its low frequency ($<5\,year^{-1}$) and the winter occurrence of this type of winds (mixing period), these episodes are expected to have a minor influence on the overall stratification pattern.

The summer PAR intensity in ECR is relatively high (*ca*. 170 $W\,m^{-2}$, Fig. 5). In aquatic systems located at mid-latitudes such as ECR, the summer daily insolation is greater than in tropical regions due to the combination of a

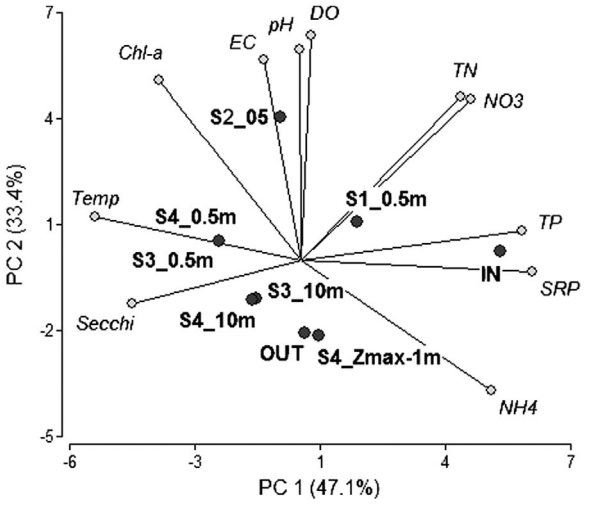

Figure 8. Biplot of sites and variables in El Carrizal reservoir. Sampling sites (in bold) are represented by red circles and the evaluated variables (in italic) by yellow circles. DO: dissolved oxygen; TN, total nitrogen; NO3, nitrate nitrogen; TP, total phosphorous: SRP, soluble reactive phosphorous; NH4, ammonia nitrogen; Secchi, Sechi disk depth; Temp, temperature; Chl-***a***, chlorophyll-***a***; EC, electrical conductivity.

longer day length and a higher angle of incidence (Kirk, 2011); however, light limitation is likely to be a significant factor controlling algal growth in ECR throughout the year (Beamud et al., 2015). Low PAR irradiation during winter coupled to mixed water column (Fig. 5) produces a narrow photic zone (Z_{Eu}:$Z_{mix} = 0.1$) and likewise, turbidity and stratification during summer also produce a relatively low Z_{Eu}:Z_{mix} ratio (0.5).

The inverse relation between Z_{SD} and Chl-***a*** in the epilimnion during both mixing and stratification coincides with the biogenic origin of turbidity (Armengol et al., 2003; Håkanson 2006). Nevertheless, the abundance of clastic sedimentary rocks in the ECR catchment and the snowmelt-controlled discharge produce higher inflow SPM during summer (León & Pedrozo, 2015), and therefore fine inorganic particulate matter may reach the photic zone and become a significant constituent of turbidity. If this phenomenon is actually taking place, the effect of projected upstream reservoirs (SRH, 2010) on river SPM transport should be addressed when considering impact on ECR trophic condition.

Twice a year ECR undergoes filling and emptying phases produced by a highly unbalanced inflow–outflow modifying the Tw temporal distribution, and as the reservoir stratifies, a spatial separation of Tw may also be expected (Pilotti et al., 2014). During water-column mixing, the reservoir acts as a completely stirred tank reactor (CSTR) where the nutrients concentration in the through-flow is equal to the concentration throughout the reservoir, and therefore the overall Tw value is representative of the system. The CSTR condition in ECR is only attained during winter, when the water column is mixed and the inflow, epilimnion, hypolimnion, and outflow densities and EC have comparable values. On the other hand, during stratification, the inflow becomes negatively buoyant producing a plunging intrusion beneath the thermocline so that the river water may be transported through the reservoir without being completely mixed with the receiving water (Morillo et al., 2006). This phenomenon is likely to produce a lower Tw in the hypolimnion than in the epilimnion due to shorter renewal time in the bottom stratum. Such hydraulic dynamics combined with a deep withdrawal may prolong summer epilimnetic Tw as a result of "short-circuiting," i.e., higher flushing rate of the inflow-hypolimnetic water (Andradóttir et al., 2012). Although the temporal dynamics of water density showed an analogous (inverse) pattern that related more to temperature than to EC, the differences between strata are higher for density than for temperature, which may indicate the EC (TDS) effect on density. It is known that the change of 1000 ppm salinity has a similar effect on water density variation as does the change of 4°C temperature (Ji, 2008); therefore, a significant influence of TDS on water density may be expected in ECR where TDS temporal variations are *ca*. 400 ppm and the highest EC values are registered at the lowest temperatures.

If it is considered that the grouping pattern observed in ECR (Fig. 8) is indicative of horizontal homogeneity, then it is possible to assume that during stratification the epilimnion volume is constant at mean thermocline depth and that minimal exchange occurs between epi and hypolimnion. This assumption enables estimating that the epilimnetic Tw during this period as approximately the number of days the reservoir remains stratified: 181 in 2009–2010; and 117 in 2010–2011. These Tw values exceed the 60–100 day threshold proposed by Søballe and Kimmel (1987) below which flushing controls phytoplankton biomass; thus, it would be possible that during the stratification period the algae advective losses may be overcome by accumulation, and the sinking rate may decrease due to turbulent mixing in the surface layer. Likewise, during mixing Chl-***a*** appeared to be related to Tw since a direct correlation was found for Tw values between 60 and 200 days (Fig. 7b). This relationship became inverse for higher values in late-winter, when minimum temperature and irradiation were recorded. As it is well known, the photosynthetic rate depends on temperature (Reynolds, 2006), therefore, the low Chl-***a*** recorded at higher Tw values may reflect the imposition of light and temperature over transport controlling algal growth.

In natural lakes, epilimnetic outflow exports warm water, whereas in reservoirs hypolimnetic withdrawal

releases cold water producing a net gain in the heat budget. The thermal structure of ECR is characterized by a deep thermocline, a wide metalimnion, and a very narrow hypolimnion confined to the deepest layers of the water column (Figs. 4 and 8). This pattern has been observed in Mediterranean reservoirs when cold hypolimnetic water is released (Moreno-Ostos et al., 2008), and may explain the low summer DO concentration at ECR deepest spots, where flux is slower and temperature is high enough for the bottom microbial community to produce anoxic sediment and release nutrients to the water column (Golterman, 2004).

4.2 Chemical factors

In River Tunuyán, the inverse correlation between TDS and discharge has been suggested to indicate dilution processes (León & Pedrozo, 2015). An analogous mechanism may be controlling TDS in ECR, which seems to propagate inside the reservoir with some degree of lag. At shorter timescales, rainfall upstream ECR showed to also affect the river flow and composition; the inflow discharge, EC, and DIN sharply increased after raining events and returned to pre-rain values within the next few days. This increment in concentration of mobile compounds related to rainfall may indicate the input of flushed sub-surface water to the river, which passes through an agricultural zone, and is therefore rich in nitrogen species and salts from flooding irrigation practices (Jones & Downing, 2009). Although the reservoir moderated the instantaneous increase of EC and DIN, the concentration increment at IN suggests that the joint magnitude of rainstorm events may have a significant influence in nutrient availability and elemental mass balance calculations. The average dissolved N input to ECR by River Tunuyán is $1.2\,\mathrm{ton\,N\,d^{-1}}$ (León, 2013), and increases approximately to $6.0\,\mathrm{ton\,N\,d^{-1}}$ after intense rainstorm.

We observed that summer epilimnetic SRSi concentrations were two orders higher in magnitude than that indicated to limit diatom growth in most lakes (Reynolds, 2006), signifying no silica limitation for diatom growth, which is also evidenced by the dominance of this group over phytoplankton (Beamud et al., 2015). The high concentration of soluble reactive silica (SRSi) is known to be a widespread water feature in the rivers draining the Andes in southern South America (Pedrozo et al., 1993; León & Pedrozo, 2015).

In ECR, the average total and dissolved concentration of phosphorus and nitrogen were higher than those estimated to limit phytoplankton primary production (Kosten et al., 2009) and only decreased to near N-limitation epilimnetic values at the end of the stratification period. This dissolved N drop is probably due to algal consumption in the surface layer; although water intrusions often supply nutrients or dilute their concentration in localized layers (Marti et al., 2011), nutrient-rich inflow plunges to deeper layers preventing epilimnetic water renewal.

The trophic state estimated from TP concentration did not correspond with observed Chl-***a*** concentration. This decoupling may have resulted from the high loads of biologically unavailable phosphorous entering the reservoir, which travel through the water body as colloidal particles (Golterman, 2004). Besides, epilimnetic Chl-***a*** variations were unrelated to SRP and NO_3^- in both the mixing and stratification periods, which may indicate that these nutrients do not limit phytoplankton growth. Nevertheless, although the annual averages of DIN and PRS in epilimnion were higher than those indicated by Kosten et al. (2009) for N and P limitation, after summer Chl-***a*** maximum, the DIN:PRS ratio decreased below the 7:1 ratio for N limitation (Reynolds, 2006) suggesting that the DIN decrease during late stratification may be produced by algae consumption as mentioned earlier, resulting in a self-limitation mechanism of phytoplankton growth. The highest Chl-***a*** was recorded at site S2, where the highest DIN:PRS ratio was recorded. This site is located within an embayment and receives high nitrogen inputs from Stream Carrizal, which is fed by subsurface inputs and irrigation surpluses from a heavily cultivated area delivering a high DIN load ($\sim 140\,\mathrm{kg\,N\,km^{-2}\,y^{-1}}$; León, 2013). It seems likely that the combination of a sheltered location ($>$Tw and $>$Temp) and a high N content results in a highly productivity environment. The phytoplankton preference for inorganic N source has been indicated to be NH_4^+ over NO_3^-, when NH_4^+ concentrations exceed $14\,\mu\mathrm{gN\,L^{-1}}$ (Reynolds, 2006). In ECR, epilimnetic concentration of NH_4^+ is close to that value, and during stratification this variable was observed to be inversely associated with Chl-***a***, suggesting that NH_4^+ consumption may be linked to biomass net accumulation, as observed by Beamud et al. (2015).

5 Conclusions

This study supports the hypothesis of the existence of alternate conditions in the water column enabling Chl-***a*** peaks to develop. Those peaks coincided with high Tw periods (Tw $>$ 100 days) produced by withdrawal interruption in winter and by epilimnion isolation (stratification) in summer. Winter Chl-***a*** maximum is likely due to increased light acquisition by water-column mixing, whereas in the summer warm and well-illuminated epilimnetic waters phytoplankton find ideal growing conditions and are only limited by nutrient depletion at the end of the stratification period due to reduced water renewal. Given that water-column stratification did seasonally affect the spatial distribution of Tw inside ECR, it is unsuitable using the

annual average of Tw to assess the effect of this hydraulic parameter on the reservoir trophic state.

The authors would like to thank G. Baffico and R. Escalante for analysis assistance; P. Bueno for laboratory support; H. Segal and A. Villodas for hydrologic data and discussion; and R. Aguilar for the English review. We also thank two anonymous reviewers whose comments and suggestions have improved the original manuscript. This study received financial support from Agencia Nacional de Promoción Científica y Tecnológica (PICT 2010–0270) and Universidad Nacional del Comahue (Program 04/B166).

The authors have declared no conflict of interest.

6 References

APHA. 1998: *Standard Methods for the Examination of Water and Wastewater*, 20th edn., American Public Health Association, Washington DC.

Andradóttir, H. Ó., Rueda, J. F., Armengol, J., Marcé, R. 2012: Characterization of residence time variability in a managed monomictic reservoir. *Water Resour. Res*. *20*, 195–210.

Antenucci, J., Imerito, A. 2000: *The CWR Dynamic Reservoir Simulation Model DYRESM. Science Manual*. Centre for Water Research, The University of Western Australia, Perth.

Armengol, J., Caputo, L., Comerma, M., Feijoó, C., et al. 2003: Sau reservoir's light climate: relationships between Secchi depth and light extinction coefficient. *Limnetica 22*, 195–210.

Beamud, S. G., León, J. G., Kruk, C., Pedrozo, F. L., Diaz, M. M. 2015: Using trait-based approaches to study phytoplankton seasonal succession in a subtropical reservoir in arid central western Argentina. *Environ. Monit. Asses*. *187*, 1–16.

Becker, V., Caputo, L., Ordóñez, J., Marcé, R., et al. 2010: Driving factors of the phytoplankton functional groups in a deep Mediterranean reservoir. *Water Res*. *44*, 3345–3354.

Carpenter, S. R., Kitchell, J. F., Hodgson, J. R., Cochran, P. A., et al. 1987: Regulation of lake primary productivity by food web structure. *Ecology 68*, 1863–1876.

Cunha, D. G. F., Calijuri, M. D. C., Lamparelli, M. C. 2013: A trophic state index for tropical/subtropical reservoirs (TSI_{tsr}). *Ecol. Eng*. *60*, 126–134.

DACC (Dirección de Agricultura y Contingencias Climáticas). 2011: Agro-meteorology. Online data: http://www.contingencias.mendoza.gov.ar/ (Accessed June 2011).

Di Rienzo, J. A., Casanove, F., Balzarini, M. G., Gonzalez, L., et al. 2013: *InfoStat Versión 2013*. Universidad Nacional de Córdoba, Córdoba.

Domingues, R. B., Barbosa, A. B., Sommer, U., Galvão, H. M. 2012: Phytoplankton composition, growth and production in the Guadiana estuary (SW Iberia): Unraveling changes induced after dam construction. *Sci. Total Environ*. *416*, 300–313.

Elçi, Ş. 2008: Effects of thermal stratification and mixing on reservoir water quality. *Limnology 9*, 135–142.

Golterman, H. L. 2004: *The Chemistry of Phosphate and Nitrogen Compounds in Sediments*. Kluwer Academic Publishers, London.

Håkanson, L. 2006: The relationship between salinity, suspended particulate matter and water clarity in aquatic systems. *Ecol. Res*. *21*, 75–90.

Hu, R., Li, Q., Han, B. P., Naselli-Flores, L., et al. 2016: Tracking management-related water quality alterations by phytoplankton assemblages in a tropical reservoir. *Hydrobiologia 763*(1), 109–124.

Ji, Z. G. 2008: *Hydrodynamics and Water Quality: Modeling Rivers, Lakes, and Estuaries*. Wiley-Interscience, New Jersey.

Jones, J, Downing, J. 2009: in: Likens, G. E. (ed.), *Encyclopedia of Inland Waters*. Elsevier, Amsterdam, pp. 225–233.

Kimmel, B. L., Lind, O. T., Paulson, L. J. 1990: in: Thornton, K.W., Kimmel, B.L., Payne, F.E. (eds.), *Reservoir Limnology: Ecological Perspectives*. John Wiley & Sons, New York, pp. 133–193.

Kirk, J. T. 2011: *Light and Photosynthesis in Aquatic Ecosystems*. Cambridge University Press, Cambridge.

Kosten, S., Huszar, V. L., Mazzeo, N., Scheffer, M., et al. 2009: Lake and watershed characteristics rather than climate influence nutrient limitation in shallow lakes. *Ecol. Appl*. *19*, 1791–1804.

León J.G. 2013: Nutrient Dynamics Effect on Phytoplankton in Embalse El Carrizal, Mendoza, Argentina: Relationship with Water Quality and Use. PhD Thesis, National University of Córdoba, Córdoba, Argentina.

León, J. G., Pedrozo, F. L. 2015: Lithological and hydrological controls on water composition: evaporite dissolution and glacial weathering in the south central Andes of Argentina (33°–34° S). *Hydrol. Process*. *29*, 1156–1172.

Lucas, L. V., Thompson, J. K., Brown, L. R. 2009: Why are diverse relationships observed between phytoplankton biomass and transport time? *Limnol. Oceanogr*. *54*, 381–390.

Marcé, R., Moreno-Ostos, E., Ordóñez, J., Feijoó, C. 2006: Nutrient fluxes through boundaries in the hypolimnion of Sau reservoir: Expected patterns and unanticipated processes. *Limnetica 25*, 527–540.

Marti, C. L., Mills, R., Imberger, J. 2011: Pathways of multiple inflows into a stratified reservoir: Thomson Reservoir, Australia. *Adv. Water Resour*. *34*, 551–561.

Masiokas, M. H., Villalba, R., Luckman, B. H., Mauget, S. 2010: Intra-to multidecadal variations of snowpack and streamflow records in the Andes of Chile and Argentina between 30 and 37 S. *J. Hydrometeorol*. *11*, 822–831.

Moreno-Ostos, E., Marce, R., Ordóñez, J., Dolz, J., Armengol, J. 2008: Hydraulic management drives heat budgets and temperature trends in a Mediterranean reservoir. *Int. Rev. Hydrobiol*. *93*, 131–147.

Morillo, S., Imberger, J., Antenucci, J. 2006: Modifying the residence time and dilution capacity of a reservoir by altering internal flow-paths. *Int. J. River Basin Manage*. *4*, 255–271.

Naselli-Flores, L. 2003: Man-made lakes in Mediterranean semi-arid climate: the strange case of Dr. Deep Lake and Mr. Shallow Lake. *Hydrobiologia 506*, 13–21.

Padisák, J., Barbosa, F. A. R., Koschel, R., Krienitz, L. 2003: Deep layer cyanoprokaryota maxima in temperate and tropical lakes. *Archiv Für Hydrobiologie Beiheft Adv. Limnol*. *58*, 175–199.

Padisák, J., O'Sullivan, P., Reynolds, C. S. 2005: *The Lakes Handbook: Limnology and Limnetic Ecology*. Vol. I John Wiley & Sons, New York pp. 251–308.

Pedrozo, F. L., Chillrud, S. N., Temporetti, P. F., Diaz, M. M. 1993: Chemical composition and nutrient limitation in rivers and lakes of Northern Patagonian Andes (39.5°−42° S; 71°W) (Rep. Argentina). *Verh. Internat. verein. Limnol*. *25*, 207–214.

Pilotti, M., Simoncelli, S., Valerio, G. 2014: A simple approach to the evaluation of the actual water renewal time of natural stratified lakes. *Water Resour. Res*. *504*, 2830–2849.

Quirós, R., Boveri, M. B. 1999: in: Tunidisi, J.G., Straškraba, M. (eds.), *Theoretical Reservoir Ecology and Its Applications*. Backhuiss Pub/Brazilian Academy of Sciences, São Paulo pp. 529–546.

Rangel, L. M., Silva, L. H., Rosa, P., Roland, F., Huszar, V. L. 2012: Phytoplankton biomass is mainly controlled by hydrology and phosphorus concentrations in tropical hydroelectric reservoirs. *Hydrobiologia 693*, 13–28.

Reynolds, C. S. 2006: *The Ecology of Phytoplankton*. Cambridge University Press, Cambridge.

Rigosi, A., Rueda, F. J. 2012: Hydraulic control of short-term successional changes in the phytoplankton assemblage in stratified reservoirs. *Ecol. Eng*. *44*, 216–226.

SMN (Servicio Meteorológico Nacional). 2011: *San Martín (Mendoza) Station Wind Data*. Servicio Meteorológico Nacional, Buenos Aires.

Søballe, D. M., Kimmel, B. L. 1987: A large-scale comparison of factors influencing phytoplankton abundance in rivers, lakes and impoundments. *Ecology 686*, 1943–1954.

Straškraba, M., Hocking, G. 2002: The effect of theoretical retention time on the hydrodynamics of deep river valley reservoirs. *Int. Rev. Hydrobiol*. *87*, 61–83.

SRH (Subsecretaría de Recursos Hídricos), 2010: *Los Blancos Hydroelectric Project. Province of Mendoza. In Spanish*. Presidencia de la Nación, Buenos Aires.

Thornton, K. W. 1990: in: Thornton, K. W., Kimmel, B. L., Payne, F. E. (eds.), *Reservoir Limnology: Ecological Perspectives*. John Wiley & Sons, New York, pp. 1–14.

Wüest, A., Lorke, A. 2003: Small-scale hydrodynamics in lakes. *Ann. Rev. Fluid Mech*. *35*, 373–412.

Zohary, T., Ostrovsky, I. 2011: Ecological impacts of excessive water level fluctuations in stratified freshwater lakes. *Inland Waters 1*, 47–59.

